Stability and performance of image based visual servo control using first order spherical image moments.

O. Bourquardez, Robert Mahony, Tarek Hamel, François Chaumette

Stability and performance of image based visual servo control using first order spherical image moments

Odile Bourquardez*, Robert Mahony§, Tarek Hamel¶ and François Chaumette*
*IRISA - CNRS and INRIA Rennes, France
Email: Firstname.Lastname@irisa.fr
§Dep. of Eng., Australian Nat. Univ., ACT, 0200 Australia
Email: Robert.Mahony@anu.edu.au
¶I3S - CNRS, Nice - Sophia Antipolis, France
Email: thamel@i3s.unice.fr

***Abstract*— Image moments provide an important class of image features used for image-based visual servo control. Spherical image moments have the additional desirable property that they are invariant under rotation of the camera frame. For these features one can study the local and global stability and performance of the position control independently of the rotation control. In this paper we study a range of control algorithms including the classical approximately linearising control, a recently proposed robust control based on Lyapunov function design methodology, and modifications of these designs to improve global and asymptotic performance and robustness of the schemes. The comparison of performance demonstrates that the choice of image feature and control design for image-based visual servo are each equally important and highly coupled. We finally propose a control law using a modified image feature and a Lyapunov control design that ensures global asymptotic stability and good performance equally in image space as in task space.**

I. Introduction

Visual servo algorithms have been extensively developed in the robotics field over the last ten years [4], [13], [8]. Visual servo systems may be divided into two main classes [12]: *Position-based visual servo* (PBVS) involves reconstruction of the target pose with respect to the robot and results in a Cartesian motion planning problem. This approach requires an accurate 3D model of the target, displays high sensitivity to image noise, poor robustness of pose estimation and the tendency for image features to leave the camera field of view during the task [2]. *Image-based visual servo* (IBVS) treats the problem as one of controlling features in the image plane, such that moving features to a goal configuration implicitly accomplishes the task [4], [14]. This approach does not require a 3D model of the target, is robust to camera calibration errors and can generally be implemented to ensure image features do not leave the camera field of view during the task. However, for an IBVS control system, good closed-loop behaviour in image space does not necessarily imply good transient or asymptotic behaviour in task space [2], [10]. Image moments are a useful and robust image feature for IBVS control [3]. A desirable property of image moments is their invariance properties [16]. In separate work, the invariance of first order spherical moments to rotational motion was used to extend IBVS techniques to a control design for an under-actuated dynamic model of an aerial robotic vehicle [7]. With these applications as a motivation it is now of interest to consider the full response of the closed-loop system in task and image space for IBVS control based on image moments.

In this paper we provide an analysis of image based visual servo (IBVS) control for a class of image features based on first order spherical moments. These features have been used in recent work [6] and have a number of important properties for the present study: they are invariant with respect to rotation of the camera frame allowing us to decouple the position and rotation dynamics of the servo problem. The interaction matrix is a positive definite matrix and allows one to design globally stable control laws. The goal of this paper is to investigate a range of control designs based on the proposed image feature and use this to demonstrate some important properties of visual servo control algorithms. In particular, we are interested in the properties of global asymptotic stability (GAS) and asymptotic performance of the closed-loop system. Global asymptotic stability (GAS) refers to the abstract property of a controller to stabilise the pose of the camera from any initial condition. No physical system is "actually" GAS and visual servo systems where target may be occluded, or leave the field of view, etc., are clearly never truly GAS. Nevertheless, by studying the theoretical properties of the closed-loop system, assuming that the target is always visible and well distinguished, we can say a great deal about the properties of some of the better known visual servo algorithms. Image based visual servo systems that are not GAS have fundamental instability built into their formulation. There are a number of examples of such systems in the literature [2], [11]. The question of asymptotic performance is also a key issue in the design of image based visual servo controllers. Since the dynamics of the system are controlled in image space, what guarantees do we have that the closed-loop response in task space is suitable. The most common problem that occurs is one of relative sensitivity where not all coordinates of the pose in task space converge at

equal rates. This leads to poor performance of the closed-loop system. To investigate these properties we propose a range of locally exponentially stable feedback laws defined in the image space. Analysis and experimental results are presented that demonstrate the fundamental properties of the closed-loop system for each result.

II. Image based error

In this paper we use an un-normalised first order image moment along with an inertial goal vector that allows us to fully decouple the position servo dynamics from the orientation servo dynamics.

Let $\mathcal{A}$ denote the inertial or task space reference frame and let $\mathcal{C}$ denote the camera or body-fixed reference frame. Let (U, V) denote the 2D pixel locations of observed points. Assume that an accurate camera calibration matrix K is available. A spherical camera geometry with unity radius is used for the mathematical construction in the sequel. Let p denote a point on the spherical image plane corresponding to pixels (U, V), one has

$$p = \frac{\bar{p}}{|\bar{p}|}, \quad \text{with} \quad \bar{p} = K \begin{pmatrix} U \\ V \\ f \end{pmatrix}. \tag{1}$$

Let $\mathcal{S}$ denote the observed image of a target on the camera image plane. The first order un-normalised moment (or centroid) is

$$q := \int_{p \in \mathcal{S}} p dp.$$

In practice, a common approach is to use point targets rather than continuous surfaces. Consider a point target consisting of n points $\{P_i\} \in \mathcal{C}$ corresponding to image points $\{p_i\}$. The centroid of a target is defined to be

$$q := \sum_{i=1}^{n} p_i \in \Re^3. \tag{2}$$

In both cases the centroid q is a three-dimensional number. Thanks to the spherical model, the third entry of the centroid is non-linearly related to depth of the camera from the observed target constellation. Using centroid information is an old technique in visual servo control [5], [1], [15], [9], [17], [3] even if a classical perspective model was used in all these works. Among the advantages one has that it is not necessary to match observed image points with desired features as would be necessary in classical image based visual servo control [8], and the calculation of an image centroid is highly robust to pixel noise and can be easily programmed in real-time.

For a point target comprising a finite number of image points the kinematics of the image centroid are easily verified to be [6]

$$\dot{q} = -\Omega \times q - QV, \tag{3}$$

where V and Ω are respectively the linear and angular velocity of the camera both expressed in the camera frame, and

$$Q = \sum_{i=1}^{i=n} \frac{\pi_{p_i}}{|P_i|} \tag{4}$$

where $\pi_p = (I_3 - pp^T)$ is the projection $\pi_p : \Re^3 \to T_p S^2$, the tangent space of the sphere S^2 at the point $p \in S^2$ (see Fig. 1).

Note that Q is a positive definite matrix if there are at least two different points p_i in the image space.

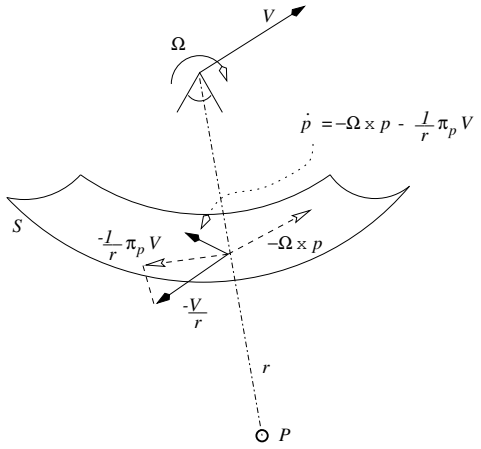

Fig. 1. Image dynamics for spherical camera geometry.

Let $b \in \mathcal{A}$ denote the fixed set point for visual feature q. The feature q is measured relative to the camera frame and not in the inertial frame, and it is necessary to map the desired set point into the camera frame before an image based error can be defined.

Let $q^* := R^\top b \in \mathcal{C}$, where rotation matrix R between the camera frame and the inertial frame is assumed to be known. That is a common assumption when dealing with the control of underactuated systems such as helicopters [6].

The image based error considered is

$$\delta := q - q^*. \tag{5}$$

The reason for choosing the image error in this manner is that it ensures the passivity-like structure of the error kinematics. That is, as we will see just below, $|\delta|$ is independent of the rotational motion, as already shown in [6].

Since $q^* \in \mathcal{C}$, it inherits dynamics from the motion of the camera: $\dot{q}^* = -\Omega \times q^*$. Thus, the image error kinematics are

$$\dot{\delta} = \delta \times \Omega - QV. \tag{6}$$

This can be written as an interaction matrix

$$\dot{\delta} = \begin{bmatrix} -Q & \delta_\times \end{bmatrix} \begin{bmatrix} V \\ \Omega \end{bmatrix}$$

where $\delta_\times$ is the skew symmetric matrix such that $\delta_\times w = \delta \times w$ for any vector w.

Taking the time derivative of $|\delta|$ and substituting for (6) yield:

$$|\dot{\delta}| = \frac{1}{|\delta|}\delta^\top \dot{\delta} = \frac{1}{|\delta|}(\delta^\top \delta_\times \Omega - \delta^\top QV)$$

A well-known property of skew symmetric matrix gives $\delta^\top \delta_\times = 0$. We finally obtain

$$|\dot{\delta}| = -\frac{\delta^\top QV}{|\delta|} \tag{7}$$

We immediately deduce that $|\delta|$ is a function of position only.

Another important property is that the image error expressed in the task space $\delta_0 := R\delta$ is a function of position only. Indeed, since $\dot{R} = R\Omega_\times$, and recalling (6) we obtain:

$$\dot{\delta_0} = R(\delta_\times \Omega - QV) + R\Omega_\times \delta = -RQV \tag{8}$$

The behaviour of δ_0 will thus not be perturbed by the camera rotational motion.

III. Image based visual servo control designs

In this section we propose a range of control design for the translational motion of the camera based on the visual feature q considered. Analysis and experimental results are presented that demonstrate the fundamental properties of the closed-loop system for each approach. System behaviour in task space and in image space, and asymptotic stability are analysed and compared.

A. Experimental conditions.

The visual feature q considered has been designed to control underactuated systems such as helicopters [7]. However in order to better compare the performance of the proposed control laws, the experiments have been realized on an holonomic six degrees of freedom robot. As can be seen on Fig. 2 the target is a four white marks on the vertices of a planar rectangle (the target size is 14×10 cm). In all the reported experiments, the initial and desired positions in 3D are the same. The desired vector q^* is chosen such that the camera set point is located at 0.5 m above the target. Fig. 2 shows the initial and goal appearance of the target. The end-effector of the robot is moved in translation according to the control law presented below. A more classical IBVS control law is used to control the rotational degrees of freedom. That is, the target centroid and its orientation in the perspective image plane are used to control these three degrees of freedom. Finally, we note that the asymptotic value Q^* of the matrix Q at the limit point is $Q^* \approx \mathrm{diag}(7.73, 7.81, 0.226)$.

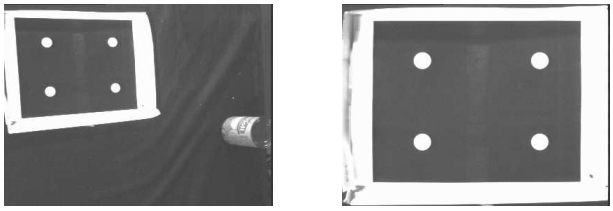

(a) (b)

Fig. 2. (a) Initial image, (b) Desired image

B. Stable control law.

This section presents a simple control law designed on Lyapunov's second theorem on stability. We obtain a globally asymptotic stable system, with non acceptable performances.

We define as storage function $\mathcal{L}$:

$$\mathcal{L} = \frac{1}{2}|\delta|^2 \tag{9}$$

From (7) we obtain immediately:

$$\dot{\mathcal{L}} = -\delta^\top QV \tag{10}$$

The matrix Q is not exactly known, however, as already said, it is known to be positive definite. Thus, a simple choice

$$V = k_\delta \delta, \quad k_\delta > 0 \tag{11}$$

is sufficient to stabilise $\mathcal{L}$. Indeed, by substituting the control input V by its expression in (10), it yields

$$\dot{\mathcal{L}} = -k_\delta \delta^\top Q \delta$$

Since Q is a positive definite matrix, classical Lyapunov theory guarantees that δ converges exponentially to zero.

Note however that the matrix Q is not well-conditioned: in the general case $\lambda_{\min}(Q) << \lambda_{\max}(Q)$. This means that convergence rates of the components of δ are not the same and the component which is affected by the eigenvalue $\lambda_{\min}(Q)$ is more sensitive to perturbations. By computing matrix Q at the desired position (Q^*), it follows that $\lambda_{\min}$ is the third eigenvalue of matrix Q. The third component of q (or δ) is thus sensitive to perturbations.

The experimental results obtained using control scheme (11) are reported on Fig. 3. We have chosen to depict $\delta_0 = R\delta$ since, as shown in (8), it is independent of the camera rotational motion, and is thus not perturbed at all by the additional control law we have used to control these rotational motion. The camera position ξ measured thanks to the robot odometry is also depicted.

We can see on Fig. 3.a that the convergence of δ_{0z} is very slow compared to the convergence of the other components δ_{0x} and δ_{0y}. Similarly, in task space, we must wait for a large number of iterations so that the depth component converges to the desired value, whereas the lateral and longitudinal components converge in few iterations (Fig. 3.b).

Although this control law ensures global asymptotic stability, the task space and image space behaviour are not suitable since convergence rates of the components are not the same.

The control schemes presented below try to compensate this sensitivity problem.

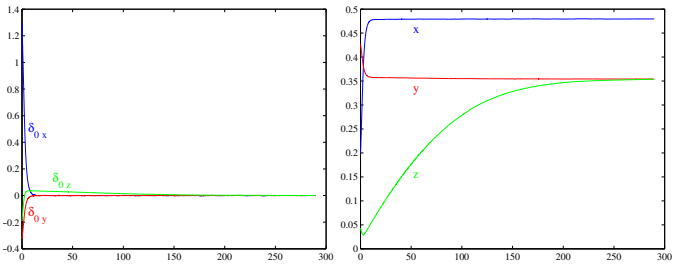

(a) (b)

Fig. 3. $V = k\delta$: time evolution of the image feature $\delta_0 = R\delta$ (a), and of the pose ξ (b) for a real experiment.

C. Classical IBVS.

The first idea for compensating the poor sensitivity in the previous control design is to use the inverse interaction matrix, as in classical IBVS. Indeed the choice $V = k_Q Q^{-1}\delta,\ k_Q > 0$ yields $\dot{\mathcal{L}} = -k_Q \delta^\top Q Q^{-1}\delta = -k_Q \delta^\top \delta$. This choice guarantees global asymptotic stability and equal convergence rates. The problem is that the matrix Q^{-1} is not exactly known, since it depends on the 3D depths $|P_i|$. In practice, we do not estimate the pose and we cannot use this control law.

The idea is then to use the *desired* interaction matrix Q^* instead of the *current* interaction matrix Q, as it is often done in classical IBVS:

$$V = k_* Q^{*-1}\delta, \quad k_* > 0 \tag{12}$$

As can be seen on Fig. 4, this control law enables equal convergence rates of the visual error components (Fig. 4.a), and equal convergence rates in task space (Fig. 4.b). However, in practice, this control scheme is adequate only in a quite small neighborhood of the desired position. Indeed we can see on Fig. 4.b that the transient behaviour of the depth z in task space is not suitable.

That is why we propose a new approach in the next section.

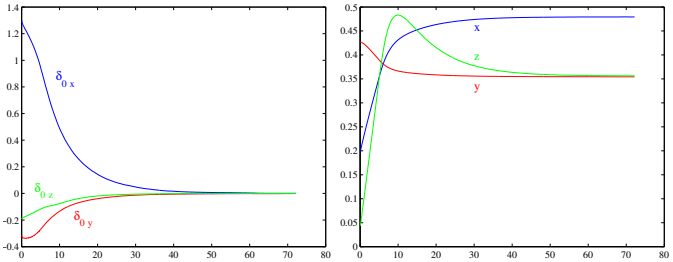

(a) (b)

Fig. 4. $V = kQ^{*-1}\delta$: time evolution of the image feature $\delta_0 = R\delta$ (a), and of the pose ξ (b) for a real experiment.

D. Rescaled image feature.

Since the fundamental problem in sensitivity comes from the nature of the image feature, it is natural to try to determine an image feature that is as close to the 3D translation between the camera and the target as possible.

A rough approximation leads to the relationship between the actual depth z from the geometric center of the target and the norm $|q|$:

$$z \propto \frac{a|q|}{\sqrt{n^2 - |q|^2}}$$

where n is the number of points observed and a is the approximate radius of the target.

From Fig. 5, we can deduce that using the centroid q to servo depth as well as lateral position works well for manoeuvres where the camera is close to the target (where the depth sensitivity is approximately linear with $|q|$). However, there is a significant loss of sensitivity as the camera moves away from the target.

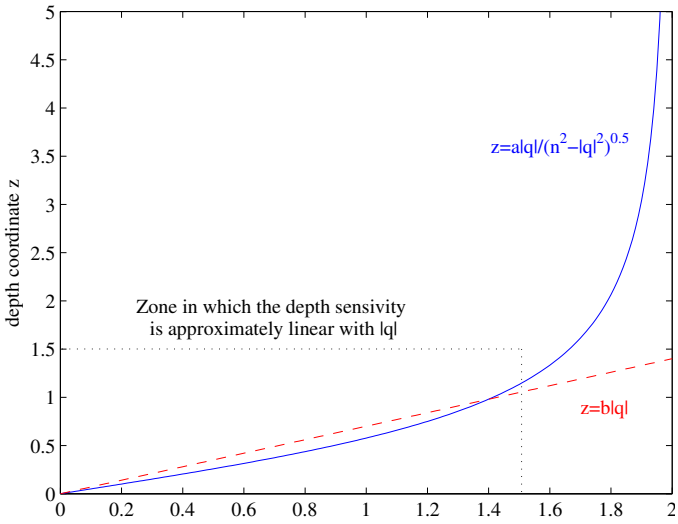

Fig. 5. Plot of the relationship between the depth z and the norm of the visual feature $|q|$ (with $a = 1$, $n = 2$). Note that for $|q| < 1.5$ then the sensitivity of the image feature to depth is approximately linear $z \approx b|q|$. For $|q| > 1.5$ the sensitivity of depth to $|q|$ is significantly reduced.

From this relationship we propose to consider as new image feature

$$f = F(|q|)q_0 \tag{13}$$

that incorporates the normalised first order moments $q_0 = \frac{q}{|q|}$ along with the scaled "depth" parameter $F(|q|)$ defined by:

$$F(|q|) := \frac{a|q|}{\sqrt{n^2 - |q|^2}} \tag{14}$$

- **Remark:** $F(|q|)$ depends on the radius of the target a. In fact this parameter acts only as a gain and the properties of the control laws presented below are preserved as long as a is positive.

The error δ_f is defined as follows

$$\delta_f = f - f^* = F(|q|)q_0 - F(|q^*|)q_0^* \tag{15}$$

Deriving (13) yields

$$\dot{f} = \frac{\partial F(|q|)}{\partial |q|}\dot{|q|}q_0 + F(|q|)\dot{q_0}$$

Using (3), we obtain after development :

$$\dot{f} = -\Omega \times f - MQV$$

where $M(q) = \frac{\partial F(|q|)}{\partial |q|}q_0 q_0^\top + \frac{F(|q|)}{|q|}\left(I_3 - q_0 q_0^\top\right)$.
Since $\dot{f^*} = -\Omega \times f^*$, we obtain immediately:

$$\dot{\delta_f} = -\Omega \times \delta_f - MQV \tag{16}$$

Taking the time derivative of the storage function $\mathcal{L} = \frac{1}{2}|\delta_f|^2$ and substituting for (16) yield:

$$\dot{\mathcal{L}} = -\delta_f^\top M(q) Q V \tag{17}$$

With the new image feature f, we have considered two control laws.

1) First control law: If we choose for the control law

$$V = k_M M \delta_f, \quad k_M > 0 \tag{18}$$

we obtain using (17) $\dot{\mathcal{L}} = -k_M \delta_f^\top M(q) Q M(q) \delta_f$. Since Q is a positive definite matrix and $M(q)$ is a symmetric and non singular matrix, classical Lyapunov theory guarantees that δ_f converges exponentially to zero.

Note that convergence rates of the components of the error δ_f are given by the eigenvalues of MQM.

- **Remark:** Let ξ denote the camera position. Classical kinematic theory gives $\dot{\xi} = \Omega \times \xi + V$. Since $\dot{f} = -\Omega \times f - MQV$ and $f \simeq -\xi$, we deduce $MQ \simeq I_3$. Thus we have $MQM \simeq Q^{-1}$.

As already said the eigenvalues of matrix Q are not the same. This means that convergence rates of the components of the error δ_f are not the same.

As can be seen on Fig. 6, components x and y converges very slowly. This is due to the fact that Q^{-1} is not well-conditioned. $\lambda_{\min}(Q)$ becomes $\lambda_{\max}(Q^{-1})$ which is the third eigenvalue of matrix Q^{-1}, and affects the z component. This situation is the opposite of the one exposed in Section III-B where the z component was affected by $\lambda_{\min}(Q)$ and converged very slowly. In the present case, the z component is affected by $\lambda_{\max}(Q^*)$ and converges very quickly with respect to the others.

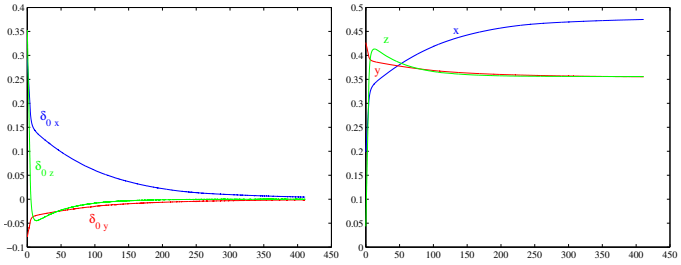

(a) (b)

Fig. 6. $V = kM\delta_f$: time evolution of the image feature $\delta_0 = R\delta$ (a), and of the pose ξ (b) for a real experiment.

Although this control law ensures global asymptotic stability, the task space and image space behaviour are not suitable since, once again, convergence rates of the components are not the same.

2) Second control law: Since $MQ \simeq I_3$ an intuitive idea is to modify the control law such that the convergence rates are given by the eigenvalues of MQ. We choose

$$V = k_f \delta_f, \quad k_f > 0 \tag{19}$$

Then recalling (17) we obtain for the derivative of the storage function: $\dot{\mathcal{L}} = -k_f \delta_f^\top M(q) Q \delta_f$.

Since $MQ \simeq I_3$, we have approximately the same convergence rate for the components of the error. Moreover we have chosen an image feature close to the 3D position: $\dot{\xi} \simeq -\dot{\delta}_f$. Thus we should obtain a good task space behaviour with same convergence rate for the components of the 3D position.

As expected the behaviour is very satisfactory in task space and in image space (Fig. 7.a and 7.b). The three components converge at equal rates, the transient behaviour is suitable, and the desired position is reached in reasonable number of iterations.

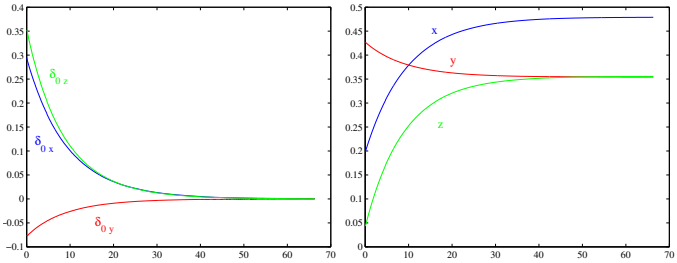

(a) (b)

Fig. 7. $V = k\delta_f$: time evolution of the image feature $\delta_0 = R\delta$ (a), and of the pose ξ (b) for a real experiment.

However the limitation of this control scheme is that we cannot demonstrate the global asymptotic stability because we are not sure to have $MQ > 0$ in all the task space.

The control we propose in the following section combines the properties we would like to ensure: good 3D behaviour, good image error convergence, and global asymptotic stability.

E. Stable control law with modified rescaled image feature.

We try to determine a new feature $g = G(|q|)q_0$ such that

$$\dot{g} = -\Omega \times g - HQV \tag{20}$$

Indeed, similar developments as in Section III-D to obtain M give the relationship between matrix H and function $G(|q|)$:

$$H(q) = \frac{\partial G(|q|)}{\partial |q|} q_0 q_0^\top + \frac{G(|q|)}{|q|}\left(I_3 - q_0 q_0^\top\right) \tag{21}$$

Note that the kinematics relationship (20) and consequently the form of matrix H in (21) have been selected to preserve the decoupling between the translational and rotational motions. Ensuring the properties we want (good 3D behaviour, good image error convergence, and global asymptotic stability) will allow us to determine H and $G(|q|)$, as explained below.

The error δ_g is defined as follows

$$\delta_g = g - g^* = G(|q|)q_0 - G(|q^*|)q_0^*$$

Recalling (20) the dynamic of this error function is given by: $\dot{\delta}_g = -\Omega \times \delta_g - HQV$.

If we choose as control law $V = k_g H(q)\delta_g$, $k_g > 0$, we obtain for the derivative of the storage function $\mathcal{L} = \frac{1}{2}|\delta_g|^2$:

$$\dot{\mathcal{L}} = -\delta_g^\top H(q) Q V = -k_g \delta_g^\top H(q) Q H(q) \delta_g \tag{22}$$

Since Q is a positive definite matrix and $H(q)$ is a symmetric and non singular matrix (see (21)), classical Lyapunov theory guarantees that δ_g converges exponentially to zero.

Since the image space convergence rates will be given by the eigenvalues of HQH, the idea is then to choose H such that HQH is well-conditioned and as near as I_3 as possible. Since $M \simeq Q^{-1}$, an intuitive choice for H is

$$H = \sqrt{M}, \tag{23}$$

since in that case we have $HQH \simeq I_3$. Finally $G(|q|)$ and thus $H(q)$ could be defined from the two equations (21) and (23).

In practice, the problem above has no solution because the constraints are too much restrictive. An intuitive idea to relax this constraints is to introduce in (23) an additional parameter $\alpha(|q|)$ such that $\alpha(|q^*|) = 1$. The new form of matrix H is given by $H = \alpha(|q|)\sqrt{M}$. We obtain after developments

$$G(|q|) \quad = \quad \alpha(|q|)\sqrt{|q|F(|q|)} \tag{24}$$

with $\alpha(|q|) = C(n, |q^*|)\frac{D^{\frac{1}{4}}}{|q|}\sqrt{\frac{n-\sqrt{D}}{n+\sqrt{D}}}$, where $D = n^2 - |q|^2$, $C(n, |q^*|)$ is chosen such that $\alpha(|q^*|) = 1$, and $F(|q|)$ is the scaled position parameter defined by (14).

If we choose as control law

$$V = \frac{k_g}{\alpha(|q|)^2} H(q)\delta_g, \quad k_g > 0 \tag{25}$$

the derivative of the storage function is then given by

$$\dot{\mathcal{L}} = -k_g \delta_g^\top \frac{H(q)QH(q)}{\alpha(|q|)^2}\delta_g \tag{26}$$

and Lyapunov theory guarantees that δ_g converges exponentially to zero.

The image space convergence rates are given by the eigenvalues of $\frac{H(q)QH(q)}{\alpha(|q|)^2}$, and the feature δ_g has been designed such that $H(q)QH(q) \simeq \alpha(|q|)^2 I_3$ and $\alpha(|q^*|)^2 = 1$. Thus we should obtain good image space behaviour, and good task space behaviour (since the feature is designed from the position scaling $G(|q|)$).

As expected, in addition to the global asymptotic stability, this control scheme ensures suitable image space convergence as can be seen on Fig. 8.a: we have the same convergence rate for the components of the error. Moreover the link between task space and image space introduced with the position scaling $G(|q|)$ is almost linear which ensures a satisfactory 3D behaviour (see Fig. 8.b)

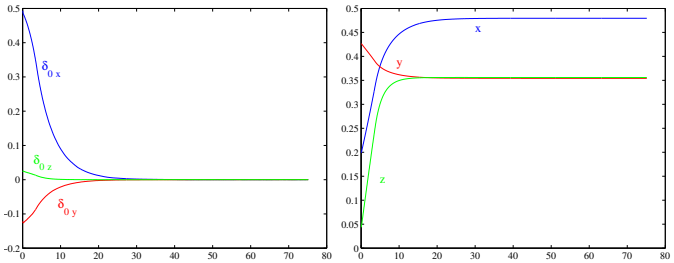

(a) (b)

Fig. 8. $V = \frac{k}{\alpha(|q|)^2} H(q)\delta_g$: time evolution of the image feature $\delta_0 = R\delta$ (a), and of the pose ξ (b) for a real experiment.

IV. Conclusion

This paper has provided an analysis of IBVS control for a class of image features based on first order spherical moments. A range of control laws defined in image space has been proposed. Analysis in terms of stability and performance has been also presented, and has been confirmed by experimental results.

A simple Lyapunov control design provides global asymptotic stability. Then modifications (based on classical IBVS) allow to improve asymptotic task and image space behaviour. But even if the control is asymptotically stable, transient behaviour in task space is not suitable. Thus we design a new image feature to have a better link between task space and image space. The last control law we have proposed using this feature ensures global asymptotic stability and good performance equally in image space as in task space. An adequate design of image feature and control law allow thus to improve drastically the obtained properties with respect to simple and classical choices.

References

[1] R. L. Andersson, *A Robot Ping-Pong Player: Experiment in Real-Time Intelligent Control*, MIT Press, Cambridge, MA, USA, 1988.

[2] F. Chaumette, *Potential problems of stability and convergence in image based and position based visual servoing*, Conflux of vision and control LNCIS, number 237, pages 66–78, 1998.

[3] F. Chaumette, *Image moments: a general and useful set of features for visual servoing*, IEEE Transactions on Robotics, 20(4):713–723, 2004.

[4] B. Espiau, F. Chaumette, and P. Rives, *A new approach to visual servoing in robotics*, IEEE Transactions on Robotics and Automation, 8(3):313–326, 1992.

[5] J. Feddema, C. S. G. Lee, and O. R. Mitchell, *Weighted selection of image features for resolved rate visual feedback control*, IEEE Transactions on Robotics and Automation, 7(1):31–47, February 1991.

[6] T. Hamel and R. Mahony, *Robust visual servoing for under-actuated dynamic systems*, Proceedings of the Conference on Decision and Control, CDC'2000, pages 3933–3938, Sydney, N.S.W., Australia, 2000.

[7] T. Hamel and R. Mahony, *Visual servoing of an under-actuated dynamic rigid-body system: An image based approach*, IEEE Transactions on Robotics and Automation, 18(2):187-198, April 2002.

[8] S. Hutchinson, G. Hager, and P. Corke, *A tutorial on visual servo control*, IEEE Transactions on Robotics and Automation, 12(5):651–670, 1996.

[9] M. Lei and B. K. Ghosh, *Visually guided robotic motion tracking*, Proceedings of the thirteenth Annual Conference on Communication, Control and Computing, pages 712–721, 1992.

[10] R. Mahony, P. Corke, and F. Chaumette, *Choice of image features for depth-axis control in image based visual servo control*, International Conference on Intelligent Robotics and Systems, IROS'2002, Switzerland, 2002.

[11] R. Mahony, T. Hamel, and F. Chaumette, *A decoupled image space approach to visual servoing for a robotic manipulator*, Proceedings of the International Conference on Robotics and Automation, ICRA'2002, Washington DC, Virginia, USA, 2002.

[12] E. Malis, F. Chaumette, and S. Boudet, *2-1/2-d visual servoing*, IEEE Transactions on Robotics and Automation, 15(2):238–250, April 1999.

[13] R. Pissard-Gibollet and P. Rives, *Applying visual servoing techniques to control of a mobile hand-eye system*, Proceedings of the IEEE International Conference on Robotics and Automation, ICRA'1995, pages 166–171, Nagasaki, Japan, 1995.

[14] C. Samson, M. Le Borgne, and B. Espiau, *Robot Control: The task function approach*, The Oxford Engineering Science Series. Oxford University Press, Oxford, U.K., 1991.

[15] A. Sanderson, L. Weiss, and C. Neuman, *Dynamic sensor based control of robots with visual feedback*, IEEE Transactions on Robotics and Automation, 3:404–417, 1987.

[16] O. Tahri, F. Chaumette, *Point-based and Region-based Image Moments for Visual Servoing of Planar Objects*, IEEE Transactions on Robotics, 21(6):1116-1127, December 2005.

[17] B. Yoshimi and P. K. Allen, *Active, uncalibrated visual servoing*, Proceedings of the International Conference on Robotics and Automation, ICRA'94, pages 156–161, San Diago, CA, USA, 1994.